NOTES AND CORRESPONDENCE

The Growth of Prognostic Differences Between GLAS Model Forecasts from SAT and NOSAT Initial Conditions

R. ATLAS

Laboratory for Atmospheric Sciences, NASA/Goddard Space Flight Center, Greenbelt, MD 20771

15 April 1981 and 11 March 1982

ABSTRACT

A study of the evolution of sounding data impact in the high-resolution GLAS model forecasts from 19 February 1976 has been conducted. The significant prognostic differences which develop in this case are shown to be traceable to specific initial state differences which resulted from the assimilation of satellite-derived temperature soundings.

1. Introduction

The high-resolution GLAS model forecasts from 0000 GMT 19 February 1976 presented by Atlas *et al.* (1982) represent a case in which a significant improvement resulted from the assimilation of satellite sounding data. Comparison of the 72 h forecast from initial conditions which included satellite temperature soundings (referred to as SAT) with the 72 h forecast from initial conditions that excluded the satellite soundings (referred to as NOSAT) showed that the predicted movements of an intense surface low are similar for the first 36–48 h of the forecast, but diverge rapidly thereafter [see Figs. 4c and 4d of Atlas *et al.* (1982)]. A study has been conducted to determine 1) why the surface lows in the two forecasts suddenly diverge and move differently during the latter half of the forecast and 2) if differences in the large-scale forcing for the cyclone, at the time the two forecasts diverge, can be traced to specific initial state differences between the SAT and NOSAT systems.

To answer these questions horizontal distributions and vertical cross sections of a large number of primary variables and model-derived quantities related to the dynamics of the cyclone have been examined. Both quantitative and synoptic aspects of the flow have been considered, but the results presented here shall be restricted to the latter.

2. Evolution of sounding data impact

The initial sea-level pressure and 1000–500 mb thickness for the SAT and NOSAT forecasts from 19 February are displayed in Figs. 1a, 1b; the corresponding 300 mb height and vorticity analyses appear in Figs. 1c and 1d. Comparison of these figures reveals no substantial difference in the initial representation of the surface low located at 46°N, 132°W off the northwest coast of the United States, although the assimilation of satellite data has produced a modification of the 1000–500 mb thickness pattern. This results in a slightly enhanced variation of thermal vorticity and thermal advection across the low center in the SAT case. At 300 mb larger differences between the two initial states are evident.

The assimilation of satellite sounding data has resulted in intensification of the upper-level vorticity maximum associated with the surface low and an elimination of the vorticity trough extending southward from this maximum. There is an increase in the northerly component of the wind and the cyclonic shear of the westerly component of the wind from 40 to 47°N to the immediate west of the upper-level trough. The anticyclonic shear of the westerly wind below 40°N (wind component charts not shown) was also increased. This results in a northward shift of the upper-level vorticity advection areas in this region, such that there is stronger positive vorticity

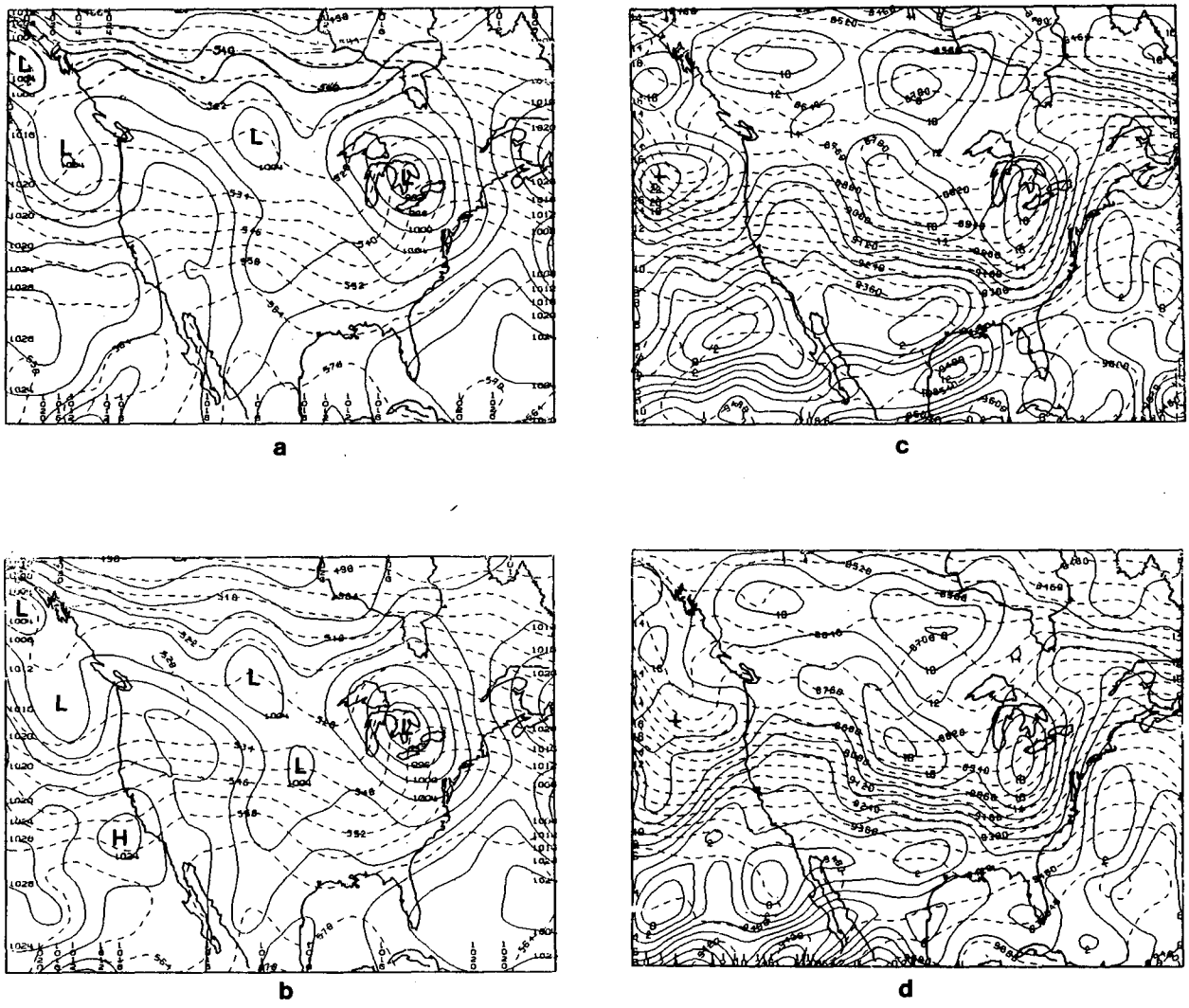

FIG. 1. Plots of sea-level pressure (solid lines) and of 1000–500 mb thickness (dashed lines) for SAT (a) and NOSAT (b) objective analyses at 0000 GMT 19 February 1976; and plots of the corresponding 300 mb absolute vorticity (solid lines) and 300 mb geopotential height (dashed lines) analyses for SAT (c) and NOSAT (d).

advection and positive vorticity tendencies to the east of the 300 mb vorticity maximum, and stronger negative vorticity advection and negative vorticity tendencies to the west of the maximum in the SAT case. This modification of the vorticity advection by satellite sounding data is in agreement with satellite cloud imagery.

Figs. 2–5 display the evolution of the sea-level pressure and 1000–500 mb thickness, as well as 300 mb height and vorticity patterns at 12 h intervals for the first 48 h of both the SAT and NOSAT predictions. During the first 12 h of the forecast, both SAT and NOSAT move the surface low inland to 46°N, 123°W (Figs. 2a, 2b). The SAT surface low has intensified while the NOSAT low has filled slightly. However, the SAT thickness gradient has weakened relative to the NOSAT and there is now a larger variation of thermal vorticity and stronger thermal vorticity advection across the low in the NOSAT case. At 300 mb a small difference in the movement of the height trough and vorticity maximum has occurred (Figs. 2c, 2d). The NOSAT vorticity maximum is located at 44°N, 128°W, while the SAT vorticity maximum has moved about 2.5° longitude further downstream. A comparison of the vorticity advection patterns and tendencies at 2 h intervals

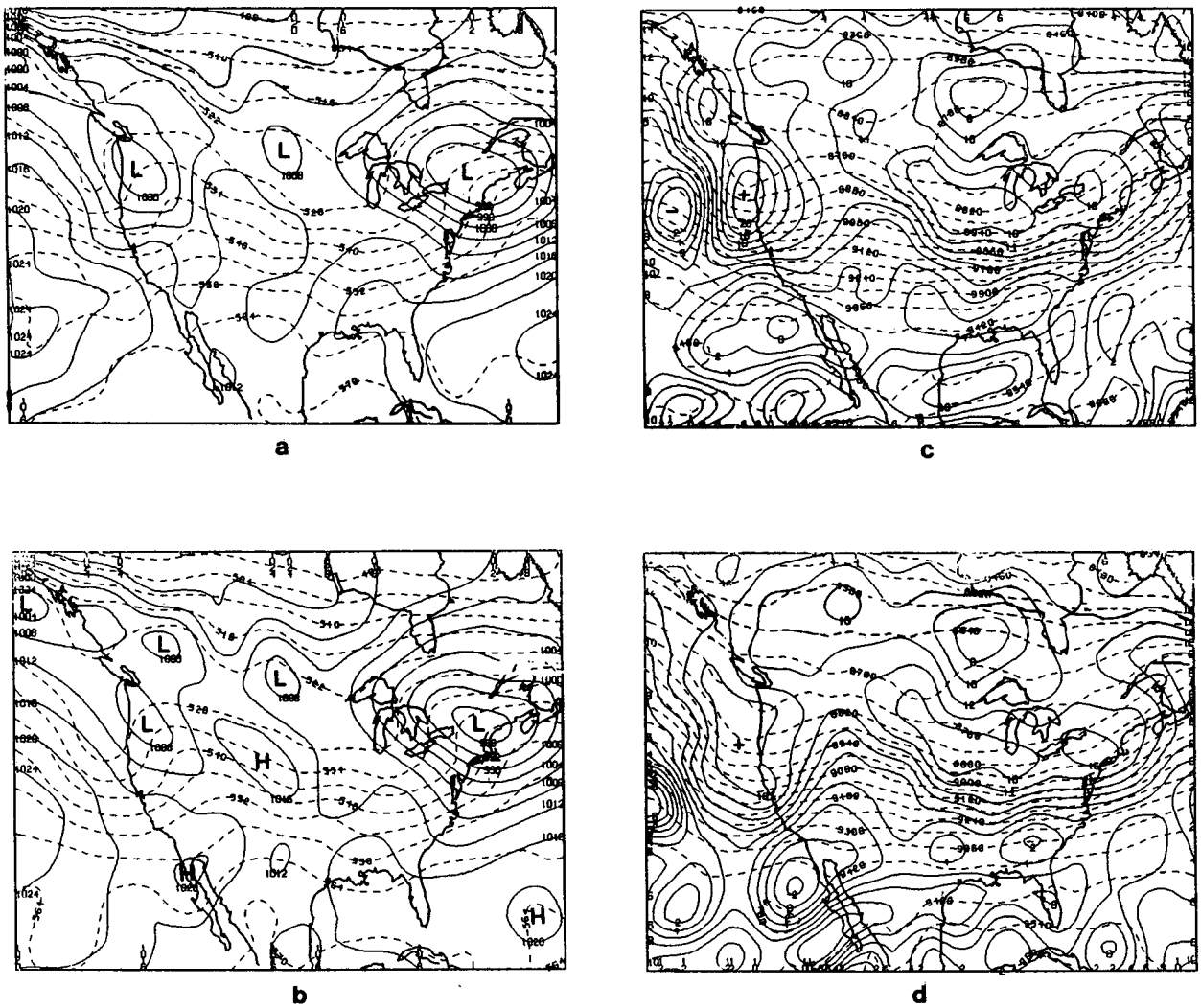

FIG. 2. As in Fig. 1, except for the 1200 GMT 19 February 1976 SAT and NOSAT forecasts from the initial state in Fig. 1.

throughout this period indicated that the initial tendency for greater movement in the SAT system has been maintained.

During the next 24 h of the forecast this trend continues and larger differences between the SAT and NOSAT systems begin to develop. At 0000 GMT 20 February (Fig. 3), the NOSAT system has forecast the surface low to deepen slightly and move to 41.3°N, 108°W, and the 300 mb vorticity maximum to move to 42°N, 123°W. The SAT system forecasts a less organized surface low with three centers evident at this time, but has maintained a somewhat stronger pressure gradient than the NOSAT to the west and southwest of the southernmost low center. SAT forecasts the 300 mb vorticity maximum to move to 41°N, 117°W, 5° longitude further downstream than the NOSAT maximum. However, in both forecasts the strongest positive vorticity advection is to the southwest of the surface low position.

By 1200 GMT 20 February the NOSAT surface low is located at 41.2°N, 105°W, while the SAT system forecasts two low centers: one at 41.2°N, 102°W; the other at 36.2°N, 102°W (Figs. 4a, 4b). Substantial differences in the low-level thermal advection patterns are also evident at this time. In the NOSAT case, there is weak cold advection directly behind the surface low, with the strongest cold advection located further southwest beneath and slightly to the west of the upper-level trough. This contributes to the deepening and slow rate of movement of the

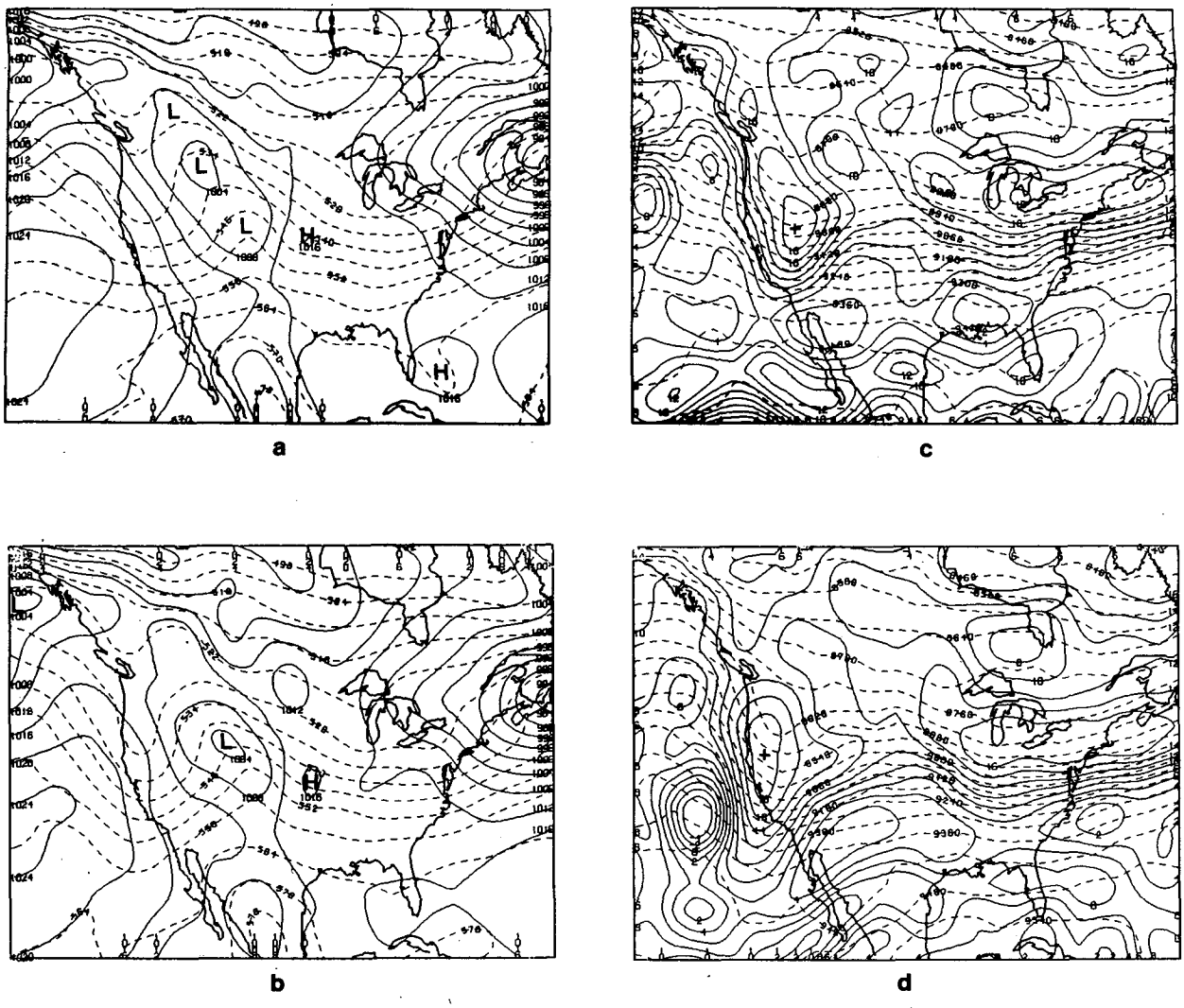

FIG. 3. As in Fig. 2, except for the 0000 GMT 20 February 1976 SAT and NOSAT forecasts from the initial state in Fig. 1.

upper-level trough in the NOSAT prediction. The SAT system predicts substantially stronger cold advection directly behind the surface low.

The relationship of low-level thermal advection to the movement of surface lows is well known (Sutcliffe, 1947; Petterssen, 1954). Warm advection contributes to falling pressure and the generation of cyclonic vorticity in advance of cyclones, while cold advection contributes to rising pressure and the destruction of cyclonic vorticity to the rear of cyclones. Thus, the gradient of thickness advection across a cyclone center is an important indicator of the rate of movement of that cyclone. In this case, the differences in the gradient of thickness advection that are established after 36 h are primarily associated with the differing rates of movement of the upper-level vorticity maximum (Figs. 4c, 4d). Because of the different movements of the vorticity maximum relative to the surface low, there was an intensification of the pressure gradient to the southwest of the low center in the SAT forecast, while a broad area of surface pressure falls associated with the positive vorticity advection aloft weakened the pressure gradient to the immediate southwest of the surface low in the NOSAT forecast.

This effect amplified during the next 12 h in such a way that by 0000 GMT 21 February the gradient of thickness advection across the low center is nearly twice as strong in the SAT forecast as in the NOSAT. At this time the surface low is located at 36.5°N, 102°W in the NOSAT forecast and at 36°N, 99°W in the SAT forecast (Figs. 5a, 5b). The 300 mb vorticity maximum is located at 36.2°N, 111°W in the NOSAT and 38°N, 102°W in the

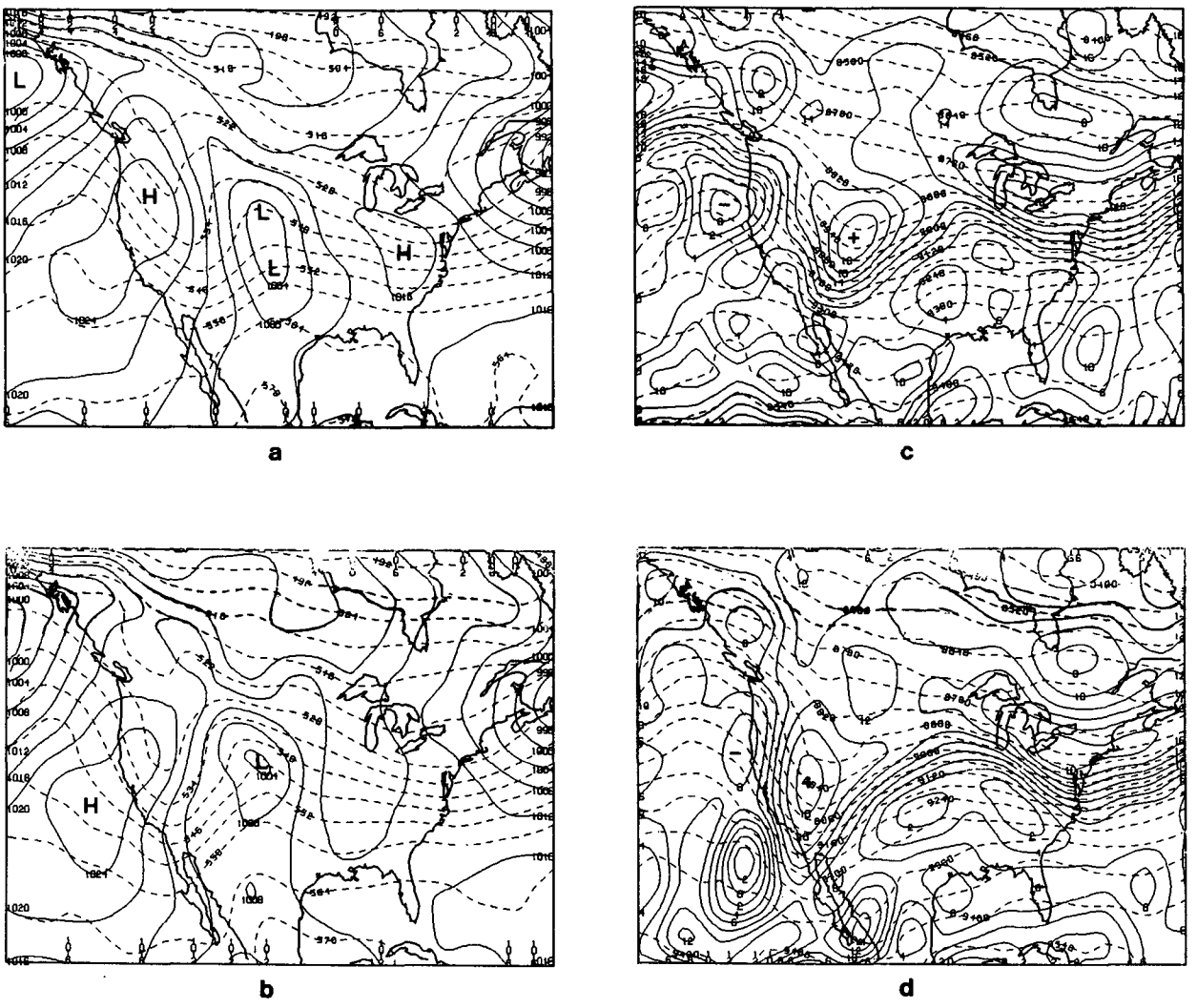

FIG. 4. As in Fig. 2, except for the 1200 GMT 20 February 1976 SAT and NOSAT forecasts from the initial state in Fig. 1.

SAT (Figs. 5c, 5d). The differing phase relationships between the upper-level vorticity maximum and the surface low coupled with the differing thickness advection patterns result in the diverging paths of the surface low throughout the remainder of the forecast. In the SAT case, there is strong positive vorticity advection and warm advection to the east and northeast of the surface low and weaker vorticity advection coupled with strong cold advection to the west and southwest of the surface low. This results in a strong isallobaric gradient across the low center, such that recurvature to the east-northeast occurs. In the NOSAT case, weak positive vorticity advection is coupled with warm advection to the northeast of the surface low, while strong positive vorticity advection is coupled with weak cold advection to the west and southwest of the surface low. As a result, the NOSAT surface low becomes "locked in" and does not progress eastward after this time.

3. Summary

This study outlines the causal chain of events which lead, from a relatively small initial state difference due to the inclusion of satellite data, to a major synoptic difference in the 72 h GLAS model forecasts from 0000 GMT 19 February 1976. The prognostic differences that resulted in diverging cyclone paths between the SAT and NOSAT forecasts were traced to initial state differences in the upper-level wind and temperature patterns. These modifications enhanced the variation of thermal vorticity and thermal advection across the cyclone center, and gave a greater initial rate of movement of the upper-

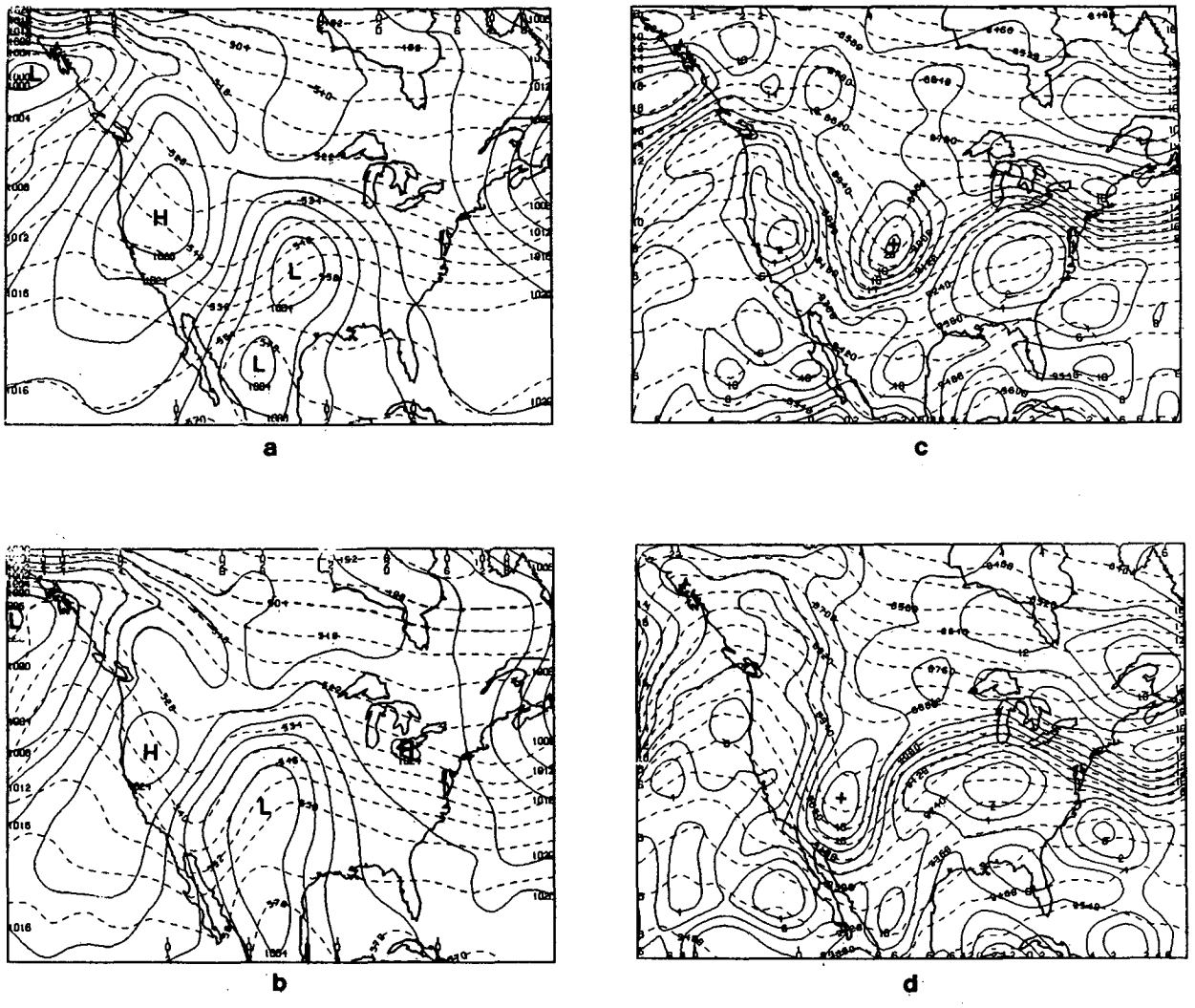

FIG. 5. As in Fig. 2, except for the 0000 GMT 21 February 1976 SAT and NOSAT forecasts from the initial state in Fig. 1.

level vorticity maximum, associated with the surface cyclone, in the SAT case.

Acknowledgments. The author wishes to acknowledge R. Rosenberg for his participation in the evaluation of sounding data impact and J. Wentz for typing the manuscript. Discussions with W. Baker, M. Ghil, M. Halem, D. R. Johnson, E. Kalnay, N. Phillips and L. Uccellini contributed to this study.

REFERENCES

Atlas, R., M. Ghil and M. Halem, 1982: The effect of model resolution and satellite sounding data on GLAS model forecasts. *Mon. Wea. Rev.*, **110**, 662–682.

Petterssen, S., 1954: A general survey of the factors influencing development at sea level. *J. Meteor.*, **122**, 36–42.

Sutcliffe, R. C. 1947: A contribution to the problem of development. *Quart. J. Roy. Meteor. Soc.*, **73**, 370–383.